Article

Photodetachment of Zwitterions: Probing Intramolecular Coulomb Repulsion and Attraction in the Gas Phase Using Mono-decarboxylated Pyridinium Dicarboxylates. Implications on the Mechanism of Orotidine 5'-Monophosphate Decarboxylase

Xue-Bin Wang, Jelena E. Dacres, Xin Yang, Lev Lis, Victoria M. Bedell, Lai-Sheng Wang, and Steven R. Kass

J. Am. Chem. Soc., **2003**, 125 (22), 6814-6826• DOI: 10.1021/ja0290835 • Publication Date (Web): 08 May 2003

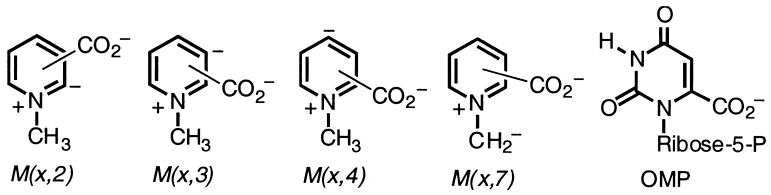

More About This Article

Additional resources and features associated with this article are available within the HTML version:

- Supporting Information
- Links to the 1 articles that cite this article, as of the time of this article download
- Access to high resolution figures
- Links to articles and content related to this article
- Copyright permission to reproduce figures and/or text from this article

View the Full Text HTML

J|A|C|S
ARTICLES
Published on Web 05/08/2003

Photodetachment of Zwitterions: Probing Intramolecular Coulomb Repulsion and Attraction in the Gas Phase Using Mono-decarboxylated Pyridinium Dicarboxylates. Implications on the Mechanism of Orotidine 5′-Monophosphate Decarboxylase

Xue-Bin Wang,[†] Jelena E. Dacres,[‡] Xin Yang,[†] Lev Lis,[‡] Victoria M. Bedell,[‡,§] Lai-Sheng Wang,*[,†] and Steven R. Kass*[,‡]

Contribution from the Department of Physics, Washington State University, 2710 University Drive, Richland, Washington 99352, W. R. Wiley Environmental Molecular Science Laboratory, MS K8-88, Pacific Northwest National Laboratory, P.O. Box 999, Richland, Washington 99352, and Department of Chemistry, University of Minnesota, Minneapolis, Minnesota 55455

Received October 24, 2002; E-mail: kass@chem.umn.edu

Abstract: Negative ion photoelectron spectra resulting from the decarboxylation of nine zwitterionic pyridinium dicarboxylates ($D(x,y)$) are reported. Structural assignments are made on the basis of analogy to the spectra of related species, labeling experiments with ^{13}C- or ^{2}H-containing substrates, independent syntheses, and comparison to density functional theory and ab initio (B3LYP and CCSD(T), respectively) results. In some cases, an acid-catalyzed isomerization of the $D(x,y)-CO_2$ ions was found to take place. Adiabatic detachment energies of the resulting zwitterionic ions were measured and are well reproduced by theory. The relative stabilities of the $D(x,y)-CO_2$ decarboxylation products are largely determined by their intramolecular electrostatic interactions, which are directly probed by the photoelectron spectra and were analyzed in terms of the resulting Coulombic forces. Expulsion of carbon dioxide from the $D(x,y)$ ions was also used as an electrostatic model to probe the mechanism of the enzyme-catalyzed conversion of orotidine 5′-monophosphate (OMP) to uridine 5′-monophosphate (UMP). It was found that the loss of CO_2 from these zwitterions and from oxygen-protonated OMP is retarded by the presence of an additional anionic group. This suggests that the formation of a zwitterion intermediate in the enzyme-catalyzed transformation of OMP to UMP may have less of an energetic impact than commonly thought and could be a "red herring". If so, the electrostatic stress mechanism proposed by Larsen et al. and Pai, Guo, and co-workers maybe followed.

Introduction

Zwitterions are useful species in a wide variety of areas including synthesis, chromatography, and the design and construction of novel materials.[1−6] Nowhere is their importance more apparent, however, than in biochemical applications where they are employed as therapeutic agents and make up much of the machinery of life. More specifically, amino acids, proteins, and enzymes exist as dipolar ions over a wide range in pH. The resulting electrostatic field plays a critical role in the structure and function of these molecules.[7−9] Despite the significance of Coulombic interactions, relatively little is known about their effect on biochemical transformations and the analysis of biomolecules via mass spectrometry.[10−18]

[†] Washington State University and Pacific Northwest National Laboratory.
[‡] University of Minnesota.
[§] University of Minnesota Supercomputer Institute Summer Undergraduate Intern.

(1) Ramos, M. J.; Melo, A.; Henriques, E. S.; Gomes, J. A. N. F.; Reuter, N.; Maigret, B.; Floriano, W. B.; Nascimento, M. A. C. *Int. J. Quantum Chem.* **1999**, *74*, 299−314.
(2) Spencer, T. A.; Onofrey, T. J.; Cann, R. O.; Russel, J. S.; Lee, L. E.; Blanchard, D. E.; Castro, A.; Gu, P.; Jiang, G.; Shechter, I. *J. Org. Chem.* **1999**, *64*, 807−818.
(3) Biegle, A.; Mathis, A.; Galin, J.-C. *Macromol. Chem. Phys.* **1999**, *200*, 1393−1406.
(4) Gothelf, K. V.; Jorgensen, K. A. *Chem. Rev.* **1998**, *98*, 863−909.
(5) Theodore, T. R.; Van Zandt, R. L.; Carpenter, R. H. *Cancer Biother. Radiopharm.* **1997**, *12*, 351−353.
(6) Caron, G.; Pagliara, A.; Gaillard, P.; Carrupt, P.-A.; Testa, B. *Helv. Chim. Acta* **1996**, *79*, 1683−1695.
(7) Warshel, A. *Acc. Chem. Res.* **1981**, *14*, 284−290.
(8) Honig, B.; Nicholls, A. *Science* **1995**, *268*, 1144−1149.
(9) (a) Wu, N.; Mo, Y.; Gao, J.; Pai, E. F. *Proc. Natl. Acad. Sci. U.S.A.* **2000**, *97*, 2017−2022. (b) Miller, B. G.; Hassell, A. M.; Wolfenden, R.; Milburn, M. V.; Short, S. A. *Proc. Natl. Acad. Sci. U.S.A.* **2000**, *97*, 2011−2016. (c) Appleby, T. C.; Kinsland, C.; Begley, T. P.; Ealick, S. E. *Proc. Natl. Acad. Sci. U.S.A.* **2000**, *97*, 2005−2010.
(10) Raposo, C.; Wilcox, C. S. *Tetrahedron Lett.* **1999**, *40*, 1285−1288.
(11) Kim, E.; Paliwal, S.; Wilcox, C. S. *J. Am. Chem. Soc.* **1998**, *120*, 11192−11193.
(12) Wilcox, C. S.; Kim, E.; Romano, D.; Kuo, L. H.; Burt, A. L.; Curran, D. P. *Tetrahedron* **1995**, *51*, 621−634.
(13) Smith, P. J.; Kim, E. I.; Wilcox, C. S. *Angew. Chem., Int. Ed. Engl.* **1993**, *32*, 1648−1650.
(14) Wyttenbach, T.; Witt, M.; Bowers, M. T. *J. Am. Chem. Soc.* **2000**, *122*, 3458−3464.
(15) Freitas, M. A.; Marshall, A. G. *Int. J. Mass Spectrom.* **1999**, *182/183*, 221−231.
(16) Ewing, N. P.; Cassady, C. J. *J. Am. Soc. Mass Spectrom.* **1999**, *10*, 928−940.
(17) Schnier, P. D.; Price, W. D.; Jockusch, R. A.; Williams, E. R. *J. Am. Chem. Soc.* **1996**, *118*, 7178−7189.

10.1021/ja0290835 CCC: $25.00

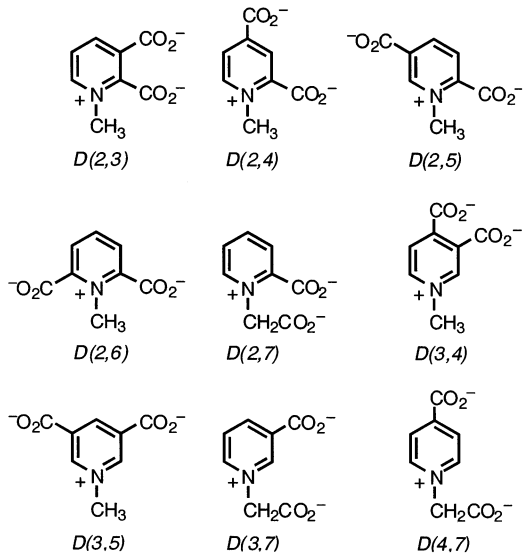

Figure 1. Dicarboxylate precursors $D(x,y)$ used in this work, where x and y indicate the locations of the two carboxylate groups.

We have recently undertaken a program to explore the reactivity and thermodynamic properties of dipolar ions in the gas phase. The first preparation, reactivity studies, and spectroscopic characterization by photoelectron spectroscopy (PES) of 1-methylpyridinium dicarboxylates and 1-carboxylatomethylpyridinium carboxylates ($D(x,y)$, Figure 1) and their nonzwitterionic counterparts were described.[19−21] In part, this was done as a prelude to investigating the consequences of electrostatic effects on biological decarboxylation reactions. This might seem odd at first, because our studies are carried out in the gas phase and most biochemical processes occur in aqueous media. However, it is well-recognized now that many enzymes provide a hydrophobic environment where the dielectric constant is small at the active site and that water is moved out of the area upon substrate binding.[22] Fundamental insights of biological significance, consequently, can be obtained from gas-phase studies.

One notable example of an important biological reaction in which electrostatic effects are universally believed to play a critical role is the decarboxylation of orotidine 5′-monophosphate (OMP) brought about by orotidine 5′-monophosphate decarboxylase (ODCase).[23−25] This transformation produces uridine 5′-monophosphate (UMP) and is the final step of de novo pyrimidine nucleotide biosynthesis (eq 1). Biologically

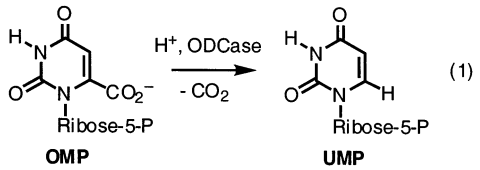

(1)

this decarboxylation is unique in that metals and cofactors do not appear to be involved even though the expulsion of carbon dioxide from OMP in a stepwise manner would lead to a localized carbanion.[26] ODCase also is remarkable in that $k_{cat}/k_{uncat} = 1.4 \times 10^{17}$ and $k_{cat}/K_m/k_{uncat} = 2.0 \times 10^{23}$ M^{-1}! This makes ODCase the most proficient enzyme currently known.[25,27] As a result, it is not surprising that the mechanism for this reaction has received an extraordinary amount of attention.[28−46] Two leading candidates for consideration have emerged. In the first group of mechanisms, protonation of OMP either at oxygen-2 or at oxygen-4 leads to a zwitterionic intermediate, which facilitates the rate-limiting decarboxylation (Scheme 1).[28,32,44,46] The second proposal involves electrostatic stress (or Jencks Circe effect)[22a] in that the decarboxylation is accelerated by the close proximity of an active-site carboxylate group (Scheme 2).[39,42] Binding of the substrate is energetically favorable overall because there are a variety of attractive enzyme−substrate interactions. Electrostatics is the key element in explaining the remarkable efficiency of ODCase in both sets of proposals.

In this paper we report the negative ion photoelectron spectra resulting from the decarboxylation of nine zwitterionic pyridinium dicarboxylates ($D(x,y)$). Isomerization was observed for several decarboxylated anions, and isotopically labeled (^{13}C and D) substrates were used to probe this process. Density functional theory and ab initio calculations (B3LYP and CCSD(T), respectively) were carried out on all of the 16 possible monocarboxylate $M(x,y)$ anions (Figure 2), as well as several reference compounds, and were used to assign the observed photoelectron spectra. The implications of our results on the mechanism for the enzyme-catalyzed conversion of OMP to UMP are discussed.

(18) Campbell, S.; Rodgers, M. T.; Marzluff, E. M.; Beauchamp, J. L. *J. Am. Chem. Soc.* **1995**, *117*, 12840−12854.
(19) Broadus, K. M.; Kass, S. R. *J. Am. Chem. Soc.* **2000**, *122*, 9014−9018.
(20) Wang, X. B.; Broadus, K. M.; Wang, L. S.; Kass, S. R. *J. Am. Chem. Soc.* **2000**, *122*, 8305−8306.
(21) Wang, X. B.; Dacres, J. E.; Yang, X.; Broadus, K. M.; Lis, L.; Wang, L. S.; Kass, S. R. *J. Am. Chem. Soc.* **2003**, *125*, 296−304.
(22) (a) Jencks, W. P. In *Advances in Enzymology and Related Areas of Molecular Biology*; Meister, A., Ed.; Wiley: New York, 1975; Vol. 43, pp 219−410. (b) Dewar, M. J. S. *Enzyme* **1986**, *36*, 8−20. (c) Cui, Q.; Karplus, M. *J. Phys. Chem. B* **2002**, *106*, 1768−1798. (d) Czerwinski, R. M.; Harris, T. K.; Massiah, M. A.; Mildvan, A. S.; Whitman, C. P. *Biochemistry* **2001**, *40*, 1984−1995. (e) Simonson, T.; Archontis, G.; Karplus, M. *J. Phys. Chem. B* **1999**, *103*, 6142−6156. (f) Cachau, R. E.; Garcia-Moreno, E. B. *J. Mol. Biol.* **1996**, *255*, 340−343. (g) Kanski, R.; Murray, C. J. *Tetrahedron Lett.* **1993**, *34*, 2263−2266.
(23) Liberman, I.; Kornberg, A.; Simms, E. S. *J. Biol. Chem.* **1955**, *215*, 403−415.
(24) McClard, R. W.; Black, M. J.; Livingstone, L. R.; Jones, M. E. *Biochemistry* **1980**, *19*, 4699−4706.
(25) Radzicka, A.; Wolfenden, R. *Science* **1995**, *267*, 90−93.
(26) Feng, W. Y.; Austin, T. J.; Chew, F.; Gronert, S.; Wu, W. *Biochemistry* **2000**, *39*, 1778−1783.
(27) Snider, M. J.; Wolfenden, R. *J. Am. Chem. Soc.* **2000**, *122*, 11507−11508.
(28) Beak, P.; Siegel, B. *J. Am. Chem. Soc.* **1976**, *98*, 3601−3606.
(29) Levine, H. L.; Brody, R. S.; Westheimer, F. H. *Biochemistry* **1980**, *19*, 4993−4999.
(30) Acheson, S. A.; Bell, J. B.; Jones, M. E.; Wolfenden, R. *Biochemistry* **1990**, *29*, 3198−3202.
(31) Cleland, W. W.; Kreevoy, M. M. *Science* **1994**, *264*, 1887−1890.
(32) Lee, J. K.; Houk, K. N. *Science* **1997**, *276*, 942−945.
(33) Wu, W.; Ley-han, A.; Wong, F. M.; Austin, T. J.; Miller, S. M. *Bioorg. Med. Chem. Lett.* **1997**, *7*, 2623−2628.
(34) Nakanishi, M. P.; Wu, W. *Tetrahedron Lett.* **1998**, *39*, 6271−6272.
(35) Cui, W.; DeWitt, J. G.; Miller, S. M.; Wu, W. *Biochem. Biophys. Res. Commun.* **1999**, *259*, 133−135.
(36) Miller, B. G.; Smiley, J. A.; Short, S. A.; Wolfenden, R. *J. Biol. Chem.* **1999**, *274*, 23841−23843.
(37) Smiley, J. A.; Saleh, L. *Bioorg. Chem.* **1999**, *27*, 297−306.
(38) Ehrlich, J. I.; Hwang, C.-C.; Cook, P. F.; Blanchard, J. S. *J. Am. Chem. Soc.* **1999**, *121*, 6966−6967.
(39) Wu, N.; Mo, Y.; Gao, J.; Pai, E. F. *Proc. Natl. Acad. Sci. U.S.A.* **2000**, *97*, 2017−2022. Scheme 2 given in this work is the model for our Scheme 2.
(40) Appleby, T. C.; Kinsland, C.; Begley, T. P.; Ealick, S. E. *Proc. Natl. Acad. Sci. U.S.A.* **2000**, *97*, 2005−2010.
(41) Harris, P.; Poulsen, J.-C. N.; Jensen, K. F.; Larsen, S. *Biochemistry* **2000**, *39*, 4217−4224.
(42) Gronert, S.; Feng, W. Y.; Chew, F.; Wu, W. *Int. J. Mass Spectrom.* **2000**, *195/196*, 251−258.
(43) Phillips, L. M.; Lee, J. K. *J. Am. Chem. Soc.* **2001**, *123*, 12067−12073.
(44) Miller, B. G.; Buterfoss, G. L.; Short, S. A.; Wolfenden, R. *Biochemistry* **2001**, *40*, 6227−6232.
(45) Houk, K. N.; Lee, J. K.; Tantillo, D. J.; Bahmanyar, S.; Hietbrink, B. N. *ChemBioChem* **2001**, *2*, 113−118.
(46) Miller, B. G.; Wolfenden, R. *Annu. Rev. Biochem.* **2002**, *71*, 847−885.

Scheme 1

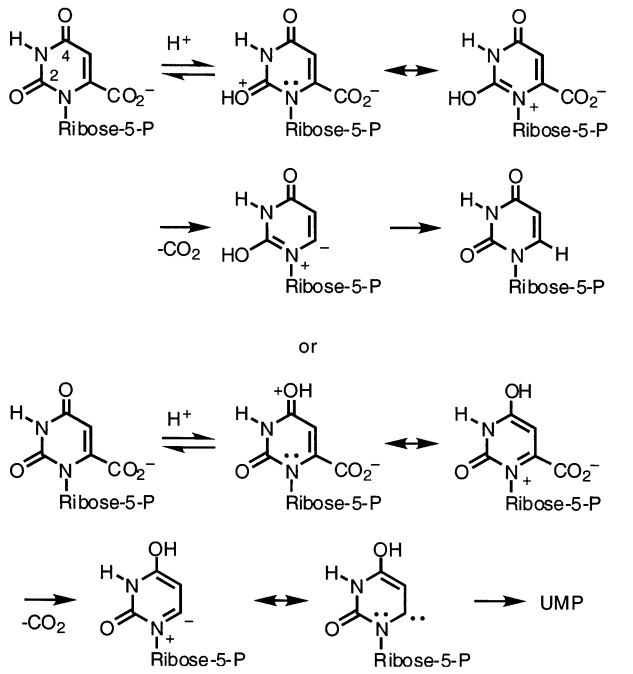

Scheme 2

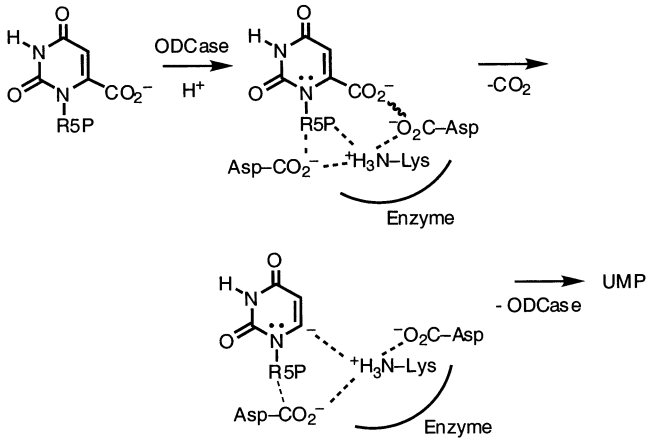

Experimental Section

Methods and Materials. Salts of 1-methylpyridiniumdicarboxylic acids, 1-carboxymethylpyridinium carboxylic acids, and 1-methyl-d_3-pyridinium-3,5-dicarboxylic acid were prepared as previously described in the literature.[19,21,47−49] Solvents were dried by standard methods, and reagents were used as received. ^{1}H and ^{13}C NMR spectra were recorded on Varian VAC-200, VAC-300, or VI-500 spectrometers and are reported in parts per million (δ).

2-Carboxy-1-carboxymethyl-2′-^{13}C-pyridinium Hydroxide, Inner Salt. Following our previously reported procedure,[21] 0.067 g (0.545 mmol) of *o*-pyridinecarboxylic acid and 0.100 g (0.714 mmol) of bromoacetic-*1*-^{13}*C* acid in 1.68 mL of water containing 4% NaOH by weight led to the formation of 0.011 g (11%) of 2-carboxy-1-carboxymethyl-*2′*-^{13}*C*-pyridinium hydroxide, inner salt: ^{1}H NMR (300 MHz, D_2O) δ 5.57 (d, J = 6.0 Hz, 2H), 8.06 (t, J = 6.9 Hz, 1H), 8.27 (d, J = 7.8 Hz, 1H), 8.64 (t, J = 7.8 Hz, 1H), 8.74 (d, J = 6.3 Hz, 1H); ^{13}C NMR (75 MHz, D_2O) δ 60.9 (d, J = 58 Hz), 128.0, 128.1, 146.8, 147.6, 150.9, 164.7, 169.7.

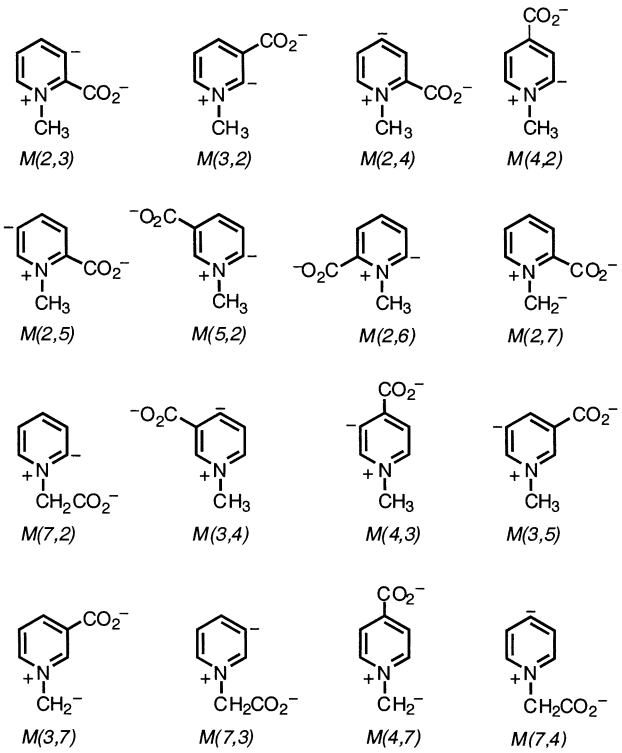

Figure 2. Zwitterionic monocarboxylate anions *M*(*x*,*y*) used in this work. The first number (*x*) provides the location of the carboxylate group, and the second number (*y*) indicates the position of the aryl anion center.

3-Carboxy-1-carboxymethyl-2′-^{13}C-pyridinium Hydroxide, Inner Salt. Following our previously reported procedure,[21] 0.050 g (0.406 mmol) of the sodium salt of *m*-pyridinecarboxylic acid, 0.075 g (0.535 mmol) of bromoacetic-*1*-^{13}C acid, and 0.070 g (0.833 mmol) of sodium bicarbonate led to the formation of 0.064 g (77%) of the sodium salt of 3-carboxy-1-carboxymethyl-2′-^{13}*C*-pyridinium hydroxide, inner salt (the addition of HCl was omitted in the workup): ^{1}H NMR (300 MHz, D_2O) δ 5.27 (d, J = 5.4 Hz, 2H), 8.10 (dd, J = 6.0 and 8.1 Hz, 1H), 8.80 (d, J = 6.0 Hz, 1H), 8.88 (d, J = 8.1 Hz, 1H), 9.10 (s, 1H); ^{13}C NMR (75 MHz, D_2O) δ 63.7 (d, J = 51 Hz), 127.8, 137.1, 145.5, 146.3, 146.5, 168.1, 171.0.

4-Carboxy-1-carboxymethyl-2′-^{13}C-pyridinium Hydroxide, Inner Salt. Following our previously reported procedure,[21] 0.050 g (0.406 mmol) of *p*-pyridinecarboxylic acid, 0.075 g (0.535 mmol) of bromoacetic-*1*-^{13}C acid, and 0.070 g (0.833 mmol) of sodium bicarbonate led to the formation of 0.054 g (65%) of the sodium salt of 4-carboxy-1-carboxymethyl-2′-^{13}*C*-pyridinium hydroxide, inner salt (the addition of HCl was omitted in the workup): ^{1}H NMR (300 MHz, D_2O) δ 5.26 (d, J = 5.4 Hz, 2H), 8.29 (d, J = 6.9 Hz, 2H), 8.83 (d, J = 6.9 Hz, 2H); ^{13}C NMR (75 MHz, D_2O) δ 63.5 (d, J = 52 Hz), 126.8, 146.3, 152.9, 169.4, 171.0.

Photoelectron Spectroscopy. A magnetic-bottle time-of-flight photoelectron spectrometer interfaced to an electrospray ion source and an ion-trap mass spectrometer was used to carry out all of the experiments reported in this study. Details of this apparatus have been described elsewhere.[50] Nine zwitterionic *D*(*x*,*y*) pyridinium dicarboxylate anions (Figure 1) were sprayed into the gas phase from 10^{-3} M water/methanol solutions (30:70 v/v) of their corresponding salts. The anions produced from the electrospray source were transported into a quadrupole ion trap, where they were accumulated for 0.1 s before

(47) (a) Lynn, D. G.; Lewis, D. H.; Tramontano, W. A.; Evans, L. S. *Phytochemistry* **1984**, *23*, 1225−1228. (b) Kristiansen, M.; Eriksen, J.; Jorgensen, K. A. *J. Chem. Soc., Perkin Trans. 1* **1990**, 101−103.
(48) (a) Lejeune, R.; Thunus, L.; Lapiere, C. L. *J. Pharm. Belg.* **1980**, *35*, 5−11. (b) Singh, A. N.; Radlowski, C. A.; Reed, J. W.; Krishnamurthy, V. V.; Gould, S. E. *Inorg. Chem.* **1981**, *20*, 211−215. (c) Kirbal, A. *Monatsh. Chem.* **1901**, *22*, 361−374. (d) Meyer, H. *Monatsh. Chem.* **1903**, *24*, 202.
(49) Kirpal, A. *Monatsh. Chem.* **1910**, *31*, 969−979.
(50) Wang, L. S.; Ding, C. F.; Wang, X. B.; Barlow, S. E. *Rev. Sci. Instrum.* **1999**, *70*, 1957−1966.

being transferred to a time-of-flight mass spectrometer. The main ion signals were from the $D(x,y)$ anions, which were the subject of a previous study.[21] Significant amounts of decarboxylated ions, $D(x,y)-CO_2$, were also produced due to collision-induced dissociation during ion transport. The signals for the decarboxylated anions were optimized by varying the voltages on the electrostatic lenses along the ion path to the quadrupole ion trap. Each anion of interest was mass selected and decelerated before being detached with a laser beam in the interaction zone of the magnetic-bottle photoelectron spectrometer. Both an excimer laser (157 and 193 nm) and an Nd:YAG laser (266 and 355 nm) were used in this study. The electron kinetic energy resolution was $\Delta E/E \sim 2\%$ (i.e., 10 meV for 0.5 eV electrons) as measured from the spectrum of I^- at 355 nm.

Computations. Geometry optimizations were carried out at the B3LYP[51] level with the 6-31+G(d) basis set on all 16 $M(x,y)$ anions and their corresponding radicals and several additional reference compounds. In one case (the $M(4,3)$ anion), the aromatic ring is not planar so MP2/6-31+G(d) and MP3/6-31+G(d) structures were computed to see if this result is an artifact of the method that was used; similar geometries were obtained from these different procedures. Vibrational frequencies were computed for each structure to ensure that they are minima on the potential energy surface and to provide zero-point energies (ZPEs). Unrestricted wave functions were used for the radicals, and, as expected, the spin contamination is small in every case. Adiabatic electron affinities (ADEs) were calculated at 0 K by taking the difference in the ZPE-corrected electronic energies of the anions and their corresponding radicals. These values were corrected for the error (0.039 eV) in the computed value for phenyl radical.

Single-point energy calculations were carried out for each compound at the B3LYP/6-311+G(2df,2pd), MP2/6-311+G(3df,2p), and CCSD(T)/6-31+G(d) levels.[52,53] The spin-unrestricted method was used again for the radical calculations except for the coupled cluster energies, which were computed using RHF-UCCSD(T) energies as implemented in MOLPRO.[54] An effective CCSD(T)/6-311+G(3df,2p) energy was subsequently obtained by taking the difference in the MP2 energies and adding it to the CCSD(T)/6-31+G(d) result (eq 2). This additivity

$$\text{CCSD(T)/6-311+G(3df,2p)} = \text{CCSD(T)/6-31+G(d)} + [\text{MP2/6-311+G(3df,2p)} - \text{MP2/6-31+G(d)}] \quad (2)$$

approach was used because the substrates of interest are too large to carry out coupled-cluster calculations directly with the large 6-311+G(3df,2p) basis set. The method that we used is analogous to G2(MP2) and G3(MP2) theory,[55,56] and its validity was tested by comparing the computed ADE of phenyl radical versus the result from the directly calculated CCSD(T)/6-311+G(3df,2p) energies. The two electron affinities are the same to within 0.07 eV, although it is worth noting that the absolute values are in poor agreement with experiment (i.e., 1.460 eV (direct calculation), 1.530 eV (additivity), and 1.096 ± 0.006 eV (expt)).[57] Nevertheless, this approach was found to reproduce the experimental electron binding energies of the $M(x,y)$ zwitterionic anions to better than 0.1 eV (see below).

All of the DFT and MP2 calculations were carried out using Gaussian 98[58] on IBM, SGI, and DEC workstations at the Minnesota Supercomputer Institute (MSI) and the Australia National University (ANU) Supercomputing Facility. CCSD(T) computations were carried out using MOLPRO[54] also at MSI and ANU because these energies are computed more efficiently with this program.

Results

Photoelectron Spectroscopy. Photoelectron spectra of the $D(x,y)-CO_2$ anions at 157 nm (7.866 eV) are shown in Figure 3. A low binding energy feature (X) is observed in each spectrum, which is not present in the spectra of the $D(x,y)$ ions.[21] The position and shape of this band appear to be the same in the 157 nm spectra for all of the $D(x,y)-CO_2$ ions except for the $D(2,6)-CO_2$ and $D(2,7)-CO_2$ isomers, which have larger and smaller binding energies, respectively. The intensities of the X feature, however, are dependent on the substrate, and it is particularly weak in the $D(2,5)-CO_2$ spectrum. The higher binding energy parts of the spectra show certain similarities to each other and to what was observed for the $D(x,y)$ zwitterions.[21] That is, both have an intense broad band with some discernible structures followed by weaker features at even higher binding energies. The strong broad band remains largely unchanged in all of the $D(x,y)-CO_2$ spectra with binding energies spanning from ~3.6 to ~5.0 eV except for that of the $D(2,6)-CO_2$ anion, which shifts to ~4.2−5.4 eV. The higher binding energy features (>5 eV) exhibit relatively weak intensities and appear to be different from species to species.

Photoelectron spectra were also obtained at three lower photon energies, 193 nm (6.424 eV), 266 nm (4.661 eV), and 355 nm (3.496 eV). The 193 and 266 nm spectra did not reveal much new information relative to the 157 nm data and are not shown here. Figure 4 shows the 355 nm spectra of eight monodecarboxylated zwitterions. At this photon energy only the X band observed in the 157 nm spectra is accessible except for the $D(2,6)-CO_2$ ion, which is too strongly bound to be interrogated by the lower energy photons. Vibrational structures are resolved in the 355 nm spectra, and significant hot band transitions are seen in the low binding energy side of the spectra. Whereas the temperature of the anions is unknown, they are expected to be only slightly above room temperature. Surprisingly, we observed that the spectra of $D(2,3)-CO_2$, $D(2,5)-CO_2$, $D(3,5)-CO_2$, and $D(3,7)-CO_2$ are identical with the same electron binding energies and vibrational structures, despite the expectation of multiple isomers. In these spectra, three vibrational features are observed due to two vibrational modes with average vibrational spacings of 520 ± 50 and 1210 ± 50 cm^{-1}, respectively. The spectra of $D(2,4)-CO_2$, $D(3,4)-CO_2$, and $D(4,7)-CO_2$ also are identical, each with a single vibrational progression and a vibrational spacing of 300 ± 50 cm^{-1}. The spectrum of $D(2,7)-CO_2$ has a smaller binding energy than the

(51) Becke, A. D. *J. Chem. Phys.* **1993**, *98*, 5648−5652.
(52) Møller, C.; Plesset, M. S. *Phys. Rev.* **1934**, *46*, 618−622.
(53) (a) Hampel, C.; Peterson, K.; Werner, H.-J. *Chem. Phys. Lett.* **1992**, *190*, 1−12. (b) Deegan, M. J. O.; Knowles, P. J. *Chem. Phys. Lett.* **1994**, *227*, 321−326. (c) Knowles, P. J.; Hampel, C.; Werner, H.-J. *J. Chem. Phys.* **1993**, *99*, 5219−5227; *J. Chem. Phys.* **2000**, *112*, 3106 (erratum).
(54) MOLPRO, a package of ab initio programs designed by Werner, H.-J. and Knowles, P. J., version 2002.1, Amos, R. D.; Bernhardsson, A.; Berning, A.; Celani, P.; Cooper, D. L.; Deegan, M. J. O.; Dobbyn, A. J.; Eckert, F.; Hampel, C.; Hetzer, G.; Knowles, P. J.; Korona, T.; Lindh, R.; Lloyd, A. W.; McNicholas, S. J.; Manby, F. R.; Meyer, W.; Mura, M. E.; Nicklass, A.; Palmieri, P.; Pitzer, R.; Rauhut, G.; Schütz, M.; Schumann, U.; Stoll, H.; Stone, A. J.; Tarroni, R.; Thorsteinsson, T.; Werner H.-J.
(55) Curtiss, L. A.; Raghavachari, K.; Trucks, G. W.; Pople, J. A. *J. Chem. Phys.* **1991**, *94*, 7221−7230.
(56) Curtiss, L. A.; Raghavachari, K.; Redfern, P. C.; Rassolov, V.; Pople, J. A. *J. Chem. Phys.* **1998**, *109*, 7764−7776.
(57) Gunion, R.; Gilles, M.; Polak, M.; Lineberger, W. C. *Int. J. Mass Spectrom. Ion Phys.* **1992**, *117*, 601−620.
(58) Frisch, M. J.; Trucks, G. W.; Schlegel, H. B.; Scuseria, G. E.; Robb, M. A.; Cheeseman, J. R.; Zakrzewski, V. G.; Montgomery, J. A., Jr.; Stratmann, R. E.; Burant, J. C.; Dapprich, S.; Millam, J. M.; Daniels, A. D.; Kudin, K. N.; Strain, M. C.; Farkas, O.; Tomasi, J.; Barone, V.; Cossi, M.; Cammi, R.; Mennucci, B.; Pomelli, C.; Adamo, C.; Clifford, S.; Ochterski, J.; Petersson, G. A.; Ayala, P. Y.; Cui, Q.; Morokuma, K.; Malick, D. K.; Rabuck, A. D.; Raghavachari, K.; Foresman, J. B.; Cioslowski, J.; Ortiz, J. V.; Stefanov, B. B.; Liu, G.; Liashenko, A.; Piskorz, P.; Komaromi, I.; Gomperts, R.; Martin, R. L.; Fox, D. J.; Keith, T.; Al-Laham, M. A.; Peng, C. Y.; Nanayakkara, A.; Gonzalez, C.; Challacombe, M.; Gill, P. M. W.; Johnson, B. G.; Chen, W.; Wong, M. W.; Andres, J. L.; Head-Gordon, M.; Replogle, E. S.; Pople, J. A. *Gaussian 98*, revision A.9; Gaussian, Inc.: Pittsburgh, PA, 1998.

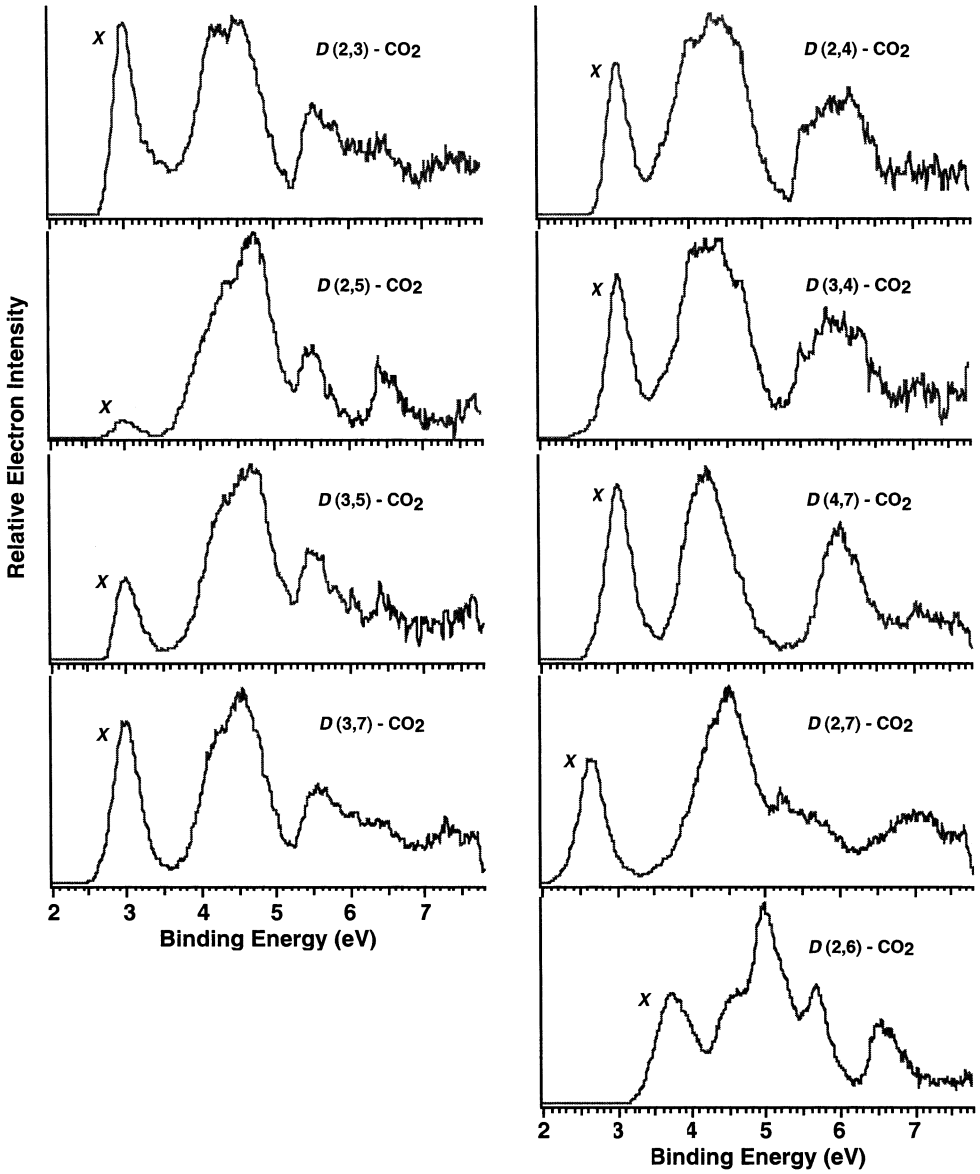

Figure 3. Photoelectron spectra at 157 nm (7.866 eV) of the zwitterionic monocarboxylate anions $M(x,y)$.

other isomers and appears to be broader with three resolved vibrational features. No vibrational structure was resolved in the spectrum of $D(2,6)-CO_2$ at 266 nm, so it is not shown here.

The adiabatic electron binding energies (ADEs) of the threshold features (X) were determined accurately from the 0−0 transitions in the 355 nm spectra (Figure 4). Because no vibrational structures were resolved for the second features (Figure 3), the corresponding ADEs were estimated by drawing a straight line along the leading edge of the respective bands and adding a constant to the intersection with the binding energy axis to account for the instrumental resolution and the finite thermal effect. The vertical electron binding energies (VDEs) were estimated from the maxima of each feature. All of the experimentally determined ADEs and VDEs measured in this work are given in Table 1.

Isotopic Substitution Studies. It should be noted that except for $D(3,5)$ and $D(2,6)$, two possible $M(x,y)$ anions can be produced from the decarboxylation of each $D(x,y)$ species as shown in Figure 2. The two potential $M(x,y)$ ions have the same mass and cannot be distinguished in our mass spectra (i.e., the PES data shown in Figures 3 and 4 could be due to both species). Certain similarities in the PES spectra for the different $M(x,y)$ ions are to be expected, but our results at 355 nm indicate that some of the $D(x,y)-CO_2$ anions have identical ADEs and vibrational structures. This strongly suggests that these species are the same and that an isomerization is taking place after the decarboxylation. To probe the structure of the fragmented products further, we studied several isotopically substituted anions. Figure 5 shows the PES spectra of two species resulting from the decarboxylation of 1-methyl-d_3-pyridinium-3,5-dicarboxylate ($M(3,5)$-d_3 and $M(3,7)$-d_2). The $M(3,5)$-d_3 anion is the direct fragmentation product of the $D(3,5)-CD_3$ parent anion, whereas the $M(3,7)$-d_2 species is the product of a proton-catalyzed reaction between $M(3,5)$-d_3 and background CH_3OH; in this transformation the carbon-centered negative charge migrates from the ring to the C7 position (methyl group) to afford the $M(3,7)$-d_2 ion and the loss of one deuterium.[19] These two ions differ in mass by 1 Da, and the d_2-isomer is ∼20% as abundant as the d_3-isomer. Despite the weaker mass signal, the 355 nm spectrum of the $M(3,7)$-d_2 ion is much stronger than

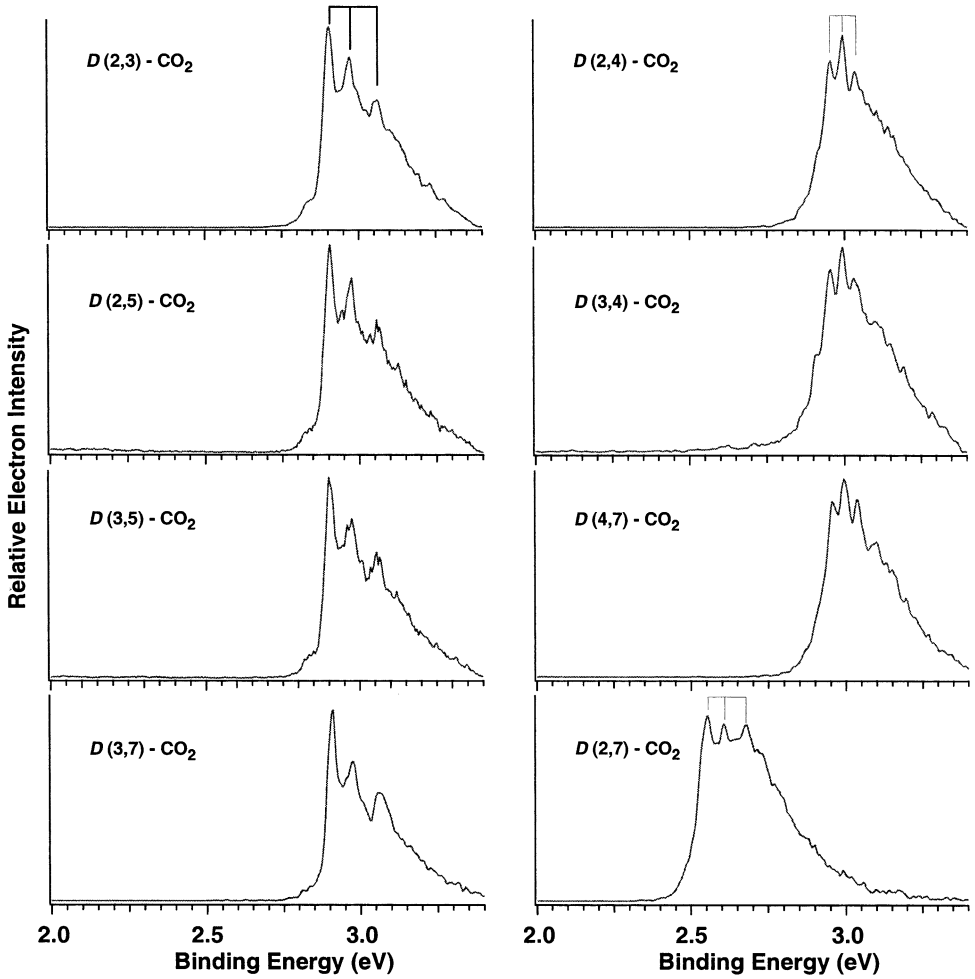

Figure 4. Photoelectron spectra at 355 nm (3.496 eV) of the zwitterionic monocarboxylate anions *M*(*x*,*y*).

Table 1. Measured Adiabatic (ADE) and Vertical (VDE) Electron Detachment Energies for the Zwitterionic *M*(*x*,*y*) Anions in eV

compd[a]	ADE (carbanion)	ADE (CO_2^-)	VDE (CO_2^-)
D(2,3)−CO_2	2.905 ± 0.010	3.8 ± 0.1	4.12 ± 0.10
D(2,4)−CO_2	2.955 ± 0.010	3.45 ± 0.10	3.95 ± 0.10
D(2,5)−CO_2	2.905 ± 0.010	3.7 ± 0.1	4.2 ± 0.1
D(2,6)−CO_2	3.38 ± 0.050	4.0 ± 0.1	4.6 ± 0.1
D(3,4)−CO_2	2.960 ± 0.010	3.35 ± 0.10	3.77 ± 0.10
D(3,5)−CO_2	2.905 ± 0.010	3.8 ± 0.1	4.2 ± 0.1
	[2.82 ± 0.05][b]		
D(2,7)−CO_2	2.555 ± 0.010	3.8 ± 0.1	3.9 ± 0.1
D(3,7)−CO_2	2.905 ± 0.010	3.94 ± 0.10	4.10 ± 0.10
D(4,7)−CO_2	2.960 ± 0.010	3.85 ± 0.10	4.22 ± 0.10

[a] See Figure 1 for the dicarboxylate *D*(*x*,*y*) precursors and Figure 2 for the zwitterionic monocarboxylate anions that might result upon the loss of carbon dioxide. [b] Unrearranged isomer; see text for additional details.

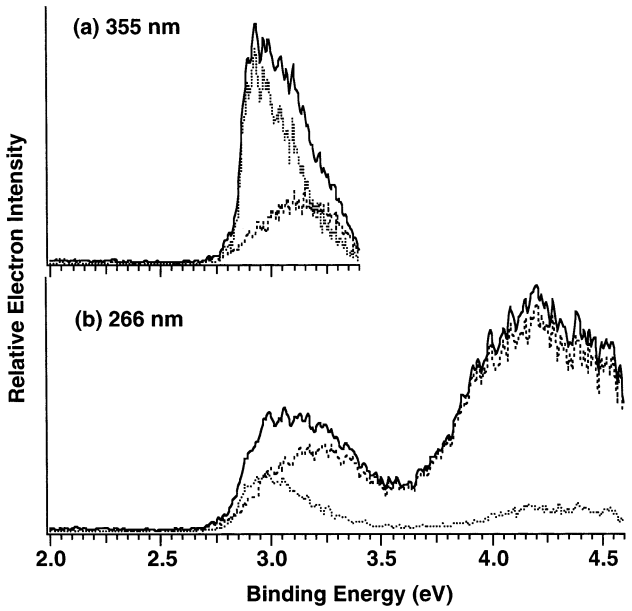

Figure 5. Normalized PES spectra of d_2-*M*(3,7) (dotted line), d_3-*M*(3,5) (dashed line), and the sum of the two (solid line) at 355 (a) and 266 nm (b).

that of the *M*(3,5)-d_3 anion taken under identical experimental conditions (i.e., photon flux and total laser shots), indicating that the *M*(3,7)-d_2 species has a larger detachment cross section at 355 nm. In contrast, at 266 nm the PES signal of the *M*(3,7)-d_2 ion is weaker than that of the *M*(3,5)-d_3 anion, which is more consistent with the relative ion abundances. Both isomers have nearly the same ADEs, but the onset for the *M*(3,7)-d_2 ion is much sharper than that for the *M*(3,5)-d_3 derivative.

We have identified that a negative charge center can isomerize from the aryl ring to the C7 methyl group. Consequently, the ^{13}C-labeled *D*(2,7), *D*(3,7), and *D*(4,7) ions (i.e., the three zwitterions with a C7 carboxylate group) were investigated to determine where the carbon dioxide is ejected from and to aid

Table 2. Observed Vibrational Frequencies for the Zwitterionic Decarboxylated $D(x,y)-CO_2$ Anions in cm^{-1}

compd[a]	frequency
$D(2,3)-CO_2$	520 ± 50, 1210 ± 50
$D(2,4)-CO_2$	300 ± 50
$D(2,5)-CO_2$	520 ± 50, 1210 ± 50
$D(2,6)-CO_2$	
$D(3,4)-CO_2$	300 ± 50
$D(3,5)-CO_2$	520 ± 50, 1210 ± 50
$D(2,7)-CO_2$	400 ± 50, 960 ± 50
$D(3,7)-CO_2$	520 ± 50, 1210 ± 50
$D(4,7)-CO_2$	300 ± 50

in the structural assignments of the $M(x,y)$ isomers. In all three cases, interestingly, we observed that the carboxylate at C7 is preferentially lost. Only for the $D(2,7)$ ion is a significant amount of decarboxylation at C2 (~40%) observed. The PES spectra reveal that the three $D(x,7)-CO_2$ ions are different from each other, and this information when combined with the isotope-labeling results indicates that the $D(3,7)-CO_2$ and $D(4,7)-CO_2$ ions are due to $M(3,7)$ and $M(4,7)$, respectively. In contrast, the $D(2,7)-CO_2$ ion maybe a mixture of the $M(2,7)$ and $M(7,2)$ species. In summary, our data at 355 nm reveal that the spectra of the $D(2,3)-CO_2$, $D(2,5)-CO_2$, and $D(3,5)-CO_2$ ions are the same as that of the $D(3,7)-CO_2$ anion and that the $D(2,4)-CO_2$ and $D(3,4)-CO_2$ isomers are the same as the $D(4,7)-CO_2$ zwitterion, indicating that the charge migration from the aryl ring to the C7 methyl group is a common isomerization path.

Computational Results. Geometry optimizations at the B3LYP level with the 6-31+G(d) basis set were carried out for all 16 $M(x,y)$ zwitterionic monocarboxylates (Figure 2) and their corresponding radicals. A summary of the structural parameters for the $M(x,y)$ anions is given in Table 3, and their three-dimensional geometries are illustrated in Figure 6. More complete details (*xyz* coordinates, absolute energies, and ZPEs) can be found in the Supporting Information.

ADEs were computed at the B3LYP/6-31+G(d) level for all 16 $M(x,y)$ anions and are given in Table 4. Single-point energy calculations also were carried out for each species at the B3LYP/6-311+G(2df,2pd) and CCSD(T)/6-311+G(3df,2p) levels; the latter results were obtained via an additivity scheme as described in the Experimental Section. The corresponding ADEs also are listed in Table 4, and the relative energies of the $M(x,y)$ zwitterions at all three levels of theory are given in Table 5. In general there is good accord between the three computational methods employed in this work.

Discussion

General Assignments of the PES Features. Figure 3 shows that the PES spectra of all of the mono-decarboxylated $D(x,y)-CO_2$ anions have a well-resolved low binding energy feature (X), a strong broad band at higher binding energies, and weaker features at even higher binding energies. The features beyond the X band correspond to detachment from the carboxylate groups and the ring π electrons of the aryl groups, respectively. As a result, these general characteristics are similar to those previously reported for benzoate, 1,2-, 1,3-, and 1,4-benzenedicarboxylate, and the zwitterionic $D(x,y)$ ions.[21,59] The low binding energy X features should (and do, see below) correspond to electron loss from the aryl or methyl anion centers in the $M(x,y)$ ions. However, a more detailed understanding of the PES data and the nature of the decarboxylated products comes from the theoretical studies.

Formation of the $D(x,y)-CO_2$ Ions and Their Subsequent Isomerization. At 355 nm, the spectra reveal vibrational structure for the threshold bands near 3 eV (Figure 4 and Table 2), which enables accurate ADEs to be determined (Table 1). Among the 10 possible $M(x,y)$ isomers that can arise from the six ring-containing $D(x,y)$ dicarboxylates (i.e., $D(2,3)$, $D(2,4)$, $D(2,5)$, $D(2,6)$, $D(3,4)$, and $D(3,5)$), only three are apparently observed. One comes from the $D(2,6)$ anion, a second isomer is formed from the $D(2,3)$, $D(2,5)$, and $D(3,5)$ zwitterions, and the third species arises from the $D(2,4)$ and $D(3,4)$ ions. The latter two have lower ADEs, which differ by only 50 meV (2.905 vs 2.955 eV), but their vibrational progressions (520 and 1210 vs 300 cm^{-1}, Table 2) are distinct. The third isomer, which comes from the $D(2,6)-CO_2$ ion, has a much higher ADE (3.38 eV), as given in Table 1. Our isotopic labeling experiments indicate that isomerizations have occurred and that the decarboxylation of the $D(2,3)$, $D(2,5)$, and *D(3,5)* ions results in the $M(3,7)$ anion, whereas the $D(2,4)$ and $D(3,4)$ zwitterions afford the $M(4,7)$ ion.

To understand the nature of the decarboxylation products and their acid-catalyzed isomerizations, we carried out extensive B3LYP and CCSD(T) calculations on all 16 possible $M(x,y)$ monocarboxylates (Figure 2). Our results indicate that even though the $D(2,3)$, $D(2,4)$, $D(2,5)$, and $D(3,4)$ isomers can lead to two different decarboxylated species (e.g., $D(2,3)-CO_2 \rightarrow M(2,3)$ and $M(3,2)$), there is a significant energetic difference between the two products (3.5−10.7 kcal mol^{-1}, Table 6)[60] and that the carboxylate which is *closer* to the formally positively charged N-center is held less tightly. This might seem to be counterintuitive because the remote carboxylate group is less affected by the positive-charge center, but any reasonable application of Coulomb's law indicates that more is gained by expulsion of the carboxylate closer to the nitrogen atom because of the greater stabilization of the resulting carbanion by the positively charged N-center. Consequently, only six $M(x,y)$ ions are expected upon fragmentation of the six ring dicarboxylates.

The computed ADEs for these species are different from each other and span from 2.355 to 3.626 eV (Table 4). These values are largely determined by the combined effects of the mutual Coulombic attraction between the oppositely charged centers and the repulsion between the two negatively charged centers. They also indicate that *some sort of rearrangement must be taking place* given the different values for the predicted ADEs. A reasonable possibility is that upon formation of the $D(x,y)-CO_2$ ions, an acid-catalyzed isomerization occurs in the presence of methanol (Scheme 3). One would then expect that the most stable isomers are produced. In the case of the $M(3,2)$, $M(5,2)$, and $M(3,5)$ ions, which come from the $D(2,3)$, $D(2,5)$, and $D(3,5)$ dicarboxylates, the most favorable rearrangement product is the $M(3,7)$ zwitterion (Table 6). This isomer can form as shown in Scheme 3 and arises by migrating the aryl anion center to the methyl group (C7). The driving force for this

(59) Wang, X. B.; Nicholas, J. B.; Wang, L. S. *J. Chem. Phys.* **2000**, *113*, 653−661.

(60) B3LYP/6-31+G(d) energies are cited in the text throughout, unless otherwise noted, because they generally are in good accord with the computationally more intensive B3LYP/6-311+G(2df,2pd) and CCSD(T)/6-311+G(3df,2p) results.

Table 3. Geometric Parameters for Zwitterionic *M*(*x*,*y*) Anions[a]

bond	*M*(2,3)	*M*(3,2)	*M*(2,4)	*M*(4,2)	*M*(2,5)	*M*(5,2)	*M*(2,6)	*M*(2,7)
N1−C2	1.378	1.372	1.368	1.376	1.361	1.377	1.374	1.428
C2−C3	1.423	1.441	1.398	1.427	1.396	1.423	1.389	1.389
C3−C4	1.403	1.391	1.419	1.391	1.397	1.390	1.397	1.400
C4−C5	1.415	1.409	1.431	1.415	1.421	1.409	1.393	1.403
C5−C6	1.374	1.373	1.377	1.370	1.391	1.376	1.415	1.373
C6−N1	1.365	1.377	1.366	1.375	1.386	1.371	1.385	1.409
$CH_{2(3)}$−N	1.475	1.471	1.471	1.469	1.476	1.472	1.478	1.341
C−CO_2	1.536	1.532	1.544	1.556	1.550	1.550	1.545	1.550
r_1	2.645		2.371	2.437	2.360	2.460	2.439	1.963
r_2					2.713	2.521		2.253
r_3					2.626			
OCCC(N)	88.4 (−88.4)[b]	99.4 (−82.6)[c]	120.0, (−60.0)[b]	0.0 (180)[d]	40.9 (−140.6)[b]	0.0 (180)[c]	121.5 (−60.0)[b]	0.0 (180)[b]

bond	*M*(7,2))	*M*(3,4)	*M*(4,3)	*M*(3,5)	*M*(3,7)	*M*(7,3)	*M*(4,7)	*M*(7,4)
N1−C2	1.379	1.366	1.397 (1.385) [1.390]	1.353	1.393	1.376	1.388	1.359
C2−C3	1.424	1.386	1.378 (1.394) [1.393]	1.387	1.380	1.400	1.381	1.384
C3−C4	1.390	1.438	1.427 (1.426) [1.431]	1.407	1.407	1.418	1.402	1.427
C4−C5	1.403	1.429	1.420 (1.416) [1.412]	1.428	1.395	1.403	1.402	1.424
C5−C6	1.381	1.383	1.377 (1.382) [1.378]	1.390	1.385	1.387	1.381	1.387
C6−N1	1.363	1.362	1.360 (1.361) [1.294]	1.384	1.387	1.351	1.388	1.357
$CH_{2(3)}$−N	1.484	1.461	1.458 (1.461) [1.511]	1.466	1.361	1.481	1.367	1.477
C−CO_2	1.578	1.552	1.525 (1.521) [1.530]	1.555	1.558	1.584	1.538	1.583
r_1	2.288	2.503	2.970 (2.821) [2.808]	2.387	2.430	2.352		2.566
r_2	2.438			2.542	2.500			
OCCC(N)	172.5 (−9.2)[e]	134.2 (−42.7)[c]	106.6 (−76.2) (113.5 (−69.7)) [115.0 (−70.3)][d,f]	179.2 (−0.7)[c]	0.0 (180)[c]	168.0 (−14.2)[e]	0.0 (180)[d]	168.3 (−13.7)[e]

[a] All distances and angles are in angstroms and degrees, respectively. The carbonyl carbon is C8, and structures are as shown in Figure 2. [b] OC8C2N1 dihedral angle. [c] OC8C3C2 dihedral angle. [d] OC8C4C3 dihedral angle. [e] OC8C7N1 dihedral angle. [f] The aromatic ring is nonplanar and has dihedral angles ranging from −3.6 to 15.2° (B3LYP), from −7.0 to 12.3° (MP2), and from −4.7 to 8.8° (MP3).

process is Coulombic in nature because C7 is directly attached to the formal positive-charge center and the methyl group is far from the remaining carboxylate center. Likewise, the *M*(4,2) and *M*(4,3) ions formed from the *D*(2,4) and *D*(3,4) dicarboxylates are converted to the *M*(4,7) isomer. As for the *M*(2,6) ion, it is stable with respect to a proton shift and does not rearrange as might be expected from simple electrostatic considerations.

The calculated ADEs for the *M*(3,7), *M*(4,7), and *M*(2,6) anions are 2.892, 2.855, and 3.244 eV, respectively, at the B3LYP/6-31+G(d) level and 2.888, 2.979, and 3.322 eV at the CCSD(T)/6-311+G(3df,2p) level (Table 4). In both cases, there is excellent agreement with the experimental ADEs of 2.905 ± 0.010 eV (*M*(3,7)), 2.955 ± 0.010 eV (*M*(4,7)), and 3.38 ± 0.05 eV (*M*(2,6)). Close examination of the 355 nm spectrum of the *D*(3,4)−CO_2 zwitterion indicates that there is a small amount of the *M*(3,7) ion present. This is understandable because the *M*(3,4) and *M*(4,3) ions differ by only 3.5 kcal mol^{-1} (i.e., one would expect the decarboxylation to be less selective in this instance, and the initial *M*(3,4) product subsequently would isomerize to the *M*(3,7) anion).

The intensity of the *X* feature in the 157 nm spectra can be rationalized by the extent to which the initially formed ions undergo isomerization. For example, the weak *X* feature of *D*(2,5)−CO_2 suggests that the majority of the decarboxylation product is the initially formed *M*(5,2) ion (computed ADE = 3.626 eV, Table 4), but its spectrum overlaps with the high binding energy features of the *M*(3,7) anion. This explanation is consistent with the small predicted *M*(5,2) → *M*(3,7) isomerization energy of −1.2 kcal mol^{-1} (−0.6 kcal mol^{-1} at the CCSD(T)/6-311+G(3df,2p) level). In contrast, the *M*(4,3) and *M*(3,4) ions formed from the *D*(3,4) anion appear to be fully converted to their *M*(4,7) and *M*(3,7) isomers because the predicted low binding energy features at 2.355 and 2.214 eV are missing in the observed spectrum of *D*(3,4)−CO_2. This is not surprising because our calculations indicate that the *M*(4,3) → *M*(4,7) and *M*(3,4) → *M*(3,7) conversions are very exothermic processes (i.e., −30.0 and −33.0 kcal mol^{-1}, respectively). As for the initially formed ions derived from the *D*(2,3), *D*(2,4), and *D*(3,5) dicarboxylates, they probably are present but either overlap or are buried under the features due to the isomerized products, as further discussed below.

Further Confirmation of the Structural Assignments and Spectral Identifications Using Isotope Labeling. To unambiguously establish our structural assignments, PES spectra of the mono-decarboxylated ions derived from independently prepared *D*(3,7) and *D*(4,7) were recorded. The observed ADE (2.905 ± 0.010 eV) and vibrational progression (520 ± 50 and 1210 ± 50 cm^{-1}) for the *D*(3,7)−CO_2 ion are identical to those obtained from the decarboxylation of the *D*(2,3), *D*(2,5), and *D*(3,5) zwitterions. Likewise, the ADE (2.960 ± 0.010 eV) and

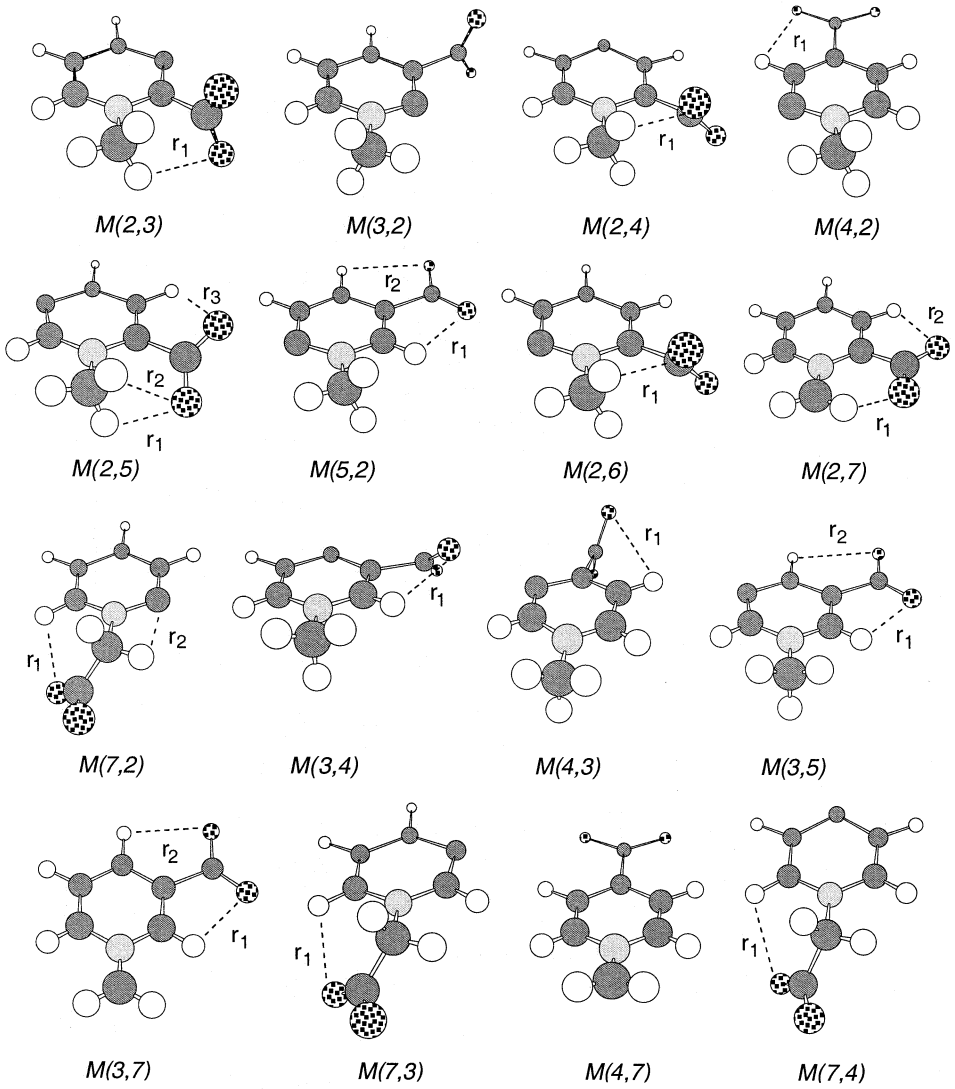

Figure 6. Computed B3LYP/6-31+G(d) geometries of zwitterionic monocarboxylates *M*(*x*,*y*).

vibrational frequency (300 ± 50 cm^{-1}) for the $D(4,7)-CO_2$ ion are the same as those obtained from the $D(2,4)-CO_2$ and $D(3,4)-CO_2$ anions. These results are in accord with our structural assignments and computational results but to ensure that the PES spectra correspond to the *M*(3,7) and *M*(4,7) anions, ^{13}C-labeled isotopomers of *D*(3,7) and *D*(4,7) were examined. In both cases, the isotopically labeled carboxylate group attached to the methylene carbon (i.e., C7) was lost exclusively upon decarboxylation. Thus, the *M*(3,7) and *M*(4,7) anions are indeed formed from the *D*(3,7) and *D*(4,7) parent ions.

The conjugate base of 1-methyl-d_3-pyridinium-3,5-dicarboxylic acid (*D*(3,5)-d_3) was also examined to further establish the methanol-catalyzed isomerization pathway (Scheme 4). In this case, the direct decarboxylation product (*M*(3,5)-d_3) is 1 Da heavier than the acid-catalyzed reaction product (*M*(3,7)-d_2), which makes it a simple matter to differentiate them by mass spectrometry. Both isomers were observed, but the d_2-ion is less abundant (~20%) than the d_3-species. If the amount of methanol in the background gas is increased, then the intensity of the d_2 ion also rises. These results confirm the acid-catalyzed pathway, but raise a new question: Why is the 355 nm spectrum of $D(3,5)-CO_2$ almost entirely due to the *M*(3,7) anion when there is a considerable amount of the *M*(3,5) isomer?[61] Control experiments using the same photon flux and total number of laser shots were carried out on *M*(3,7)-d_2 and *M*(3,5)-d_3 (Figure 5) to address this issue. We found that the signal for the former is much stronger than for the latter at 355 nm, almost assuredly because the *M*(3,7)-d_2 ion has a larger detachment cross section. The onset also is much sharper for the *M*(3,7)-d_2 ion than its *M*(3,5)-d_3 counterpart. Both of these factors result in the *M*(3,7) ion dominating the 355 nm spectrum. At 266 nm the intensities for both species are more comparable to their relative abundance.

Finally, the decarboxylation of the *D*(2,7) ion was examined. By using a ^{13}C-labeled substrate we were able to show that either carboxylate can be lost upon decarboxylation but that expulsion of the group at C7 (the methylene carbon) is favored by a factor of 2.5. This behavior is analogous to that of the *D*(3,4) ion and is consistent with our computational results, which indicate that the difference between the two pathways is only 3.1 kcal mol^{-1}. The *M*(2,7) ion probably is favored because of the conjugation between the carboxylate and the aromatic ring. Only the more abundant *M*(2,7) isomer was studied, and its ADE was measured

(61) The *M*(5,2) ion also could be present because its formation from the *M*(3,5) anion is predicted to be exothermic by 16.7 kcal mol^{-1} and would not result in a change in the deuterium content.

Table 4. Adiabatic (ADE) Electron Binding Energies for Zwitterionic Monocarboxylate *M*(*x*,*y*) Anions

	ADE[b] (eV)			
compd[a]	B3LYP/I	B3LYP/II	CCSD(T)/III	expt
M(2,3)	2.356	2.329	2.411	
M(3,2)	2.898	2.858	3.131	
M(2,4)	2.599	2.570	2.597	
M(4,2)	3.260	3.232	3.421	
M(2,5)	2.926	2.897	2.937	
M(5,2)	3.626	3.585	4.111	
M(2,6)	3.244	3.212	3.322	3.38 ± 0.050
M(3,4)	2.214	2.176	2.225	
M(4,3)	2.355	2.322	2.431	
			[2.415][c]	
M(3,5)	2.767	2.737	2.827	2.82 ± 0.05
M(2,7)	2.518	2.451	2.550	2.555 ± 0.010
M(7,2)	3.323	3.292	3.434	
M(3,7)	2.892	2.832	2.888	2.905 ± 0.010
M(7,3)	3.105	3.038	3.110	
M(4,7)	2.855	2.781	2.979	2.955 ± 0.010
M(7,4)	2.961	2.933	2.966	

[a] Zwitterionic monocarboxylate anions *M*(*x*,*y*): the first number (*x*) provides the location of the carboxylate group and the second one (*y*) indicates the position of the aryl anion center. See Figure 2 for the actual structures. [b] I = 6-31+G(d), II = 6-311+G(2df,2pd), and III = 6-311+G(3df,2p). In all three cases the single-point calculations were carried out on B3LYP/6-31+G(d) geometries and were zero-point energy corrected using unscaled vibrational frequencies at this level. B3LYP, but not CCSD(T), ADEs were corrected by adding 0.039 eV (I) and 0.045 eV (II) to account for phenyl anion's computed error. The CCSD(T) energies were obtained by additivity (see text for details). [c] In this case the CCSD(T) energy was obtained using MP3/6-31+G(d) geometries, MP3 basis set corrections, and B3LYP ZPEs.

Table 5. Relative Stabilities of Zwitterionic Monocarboxylate *M*(*x*,*y*) Anions Using B3LYP, AM1, and Coulomb's Law Calculations[a]

compd	B3LYP/I	B3LYP/II	CCSD(T)/III	AM1	Coulomb's law[b]
M(2,3)	22.7	21.8	22.0	31.7	130.7
M(3,2)	15.7	15.1	16.1	16.3	62.4
M(2,4)	15.1	14.5	14.6	23.6	120.8
M(4,2)	4.4	4.1	4.4	7.5	38.0
M(2,5)	10.5	10.1	10.1	19.2	96.2
M(5,2)	0.0	0.0	0.0	3.6	21.9
M(2,6)	0.8	0.5	0.0	0.0	0.0
M(3,4)	31.8	31.3	32.6	42.2	184.6
M(4,3)	28.3	27.6	30.4	40.1	176.3
M(3,5)	16.7	16.5	17.3	28.0	134.8
M(2,7)	1.6	−1.3	0.9	−6.8	16.6
M(7,2)	4.7	3.9	4.3	0.7	4.5
M(3,7)	−1.2	−4.1	−0.6	−6.6	14.5
M(7,3)	11.2	10.3	11.4	16.7	−13.9
M(4,7)	−1.7	−4.5	−0.7	−6.3	15.8
M(7,4)	12.3	11.3	12.4	17.9	−20.6

[a] All values in kcal mol^{-1}. All B3LYP and CCSD(T) single-point energies were carried out on B3LYP/6-31+G(d) geometries and include ZPE corrections computed at the optimization level. Basis sets are as follows: I = 6-31+G(d), II = 6-311+G(2df,2pd), and III = 6-311+G(3df,2p). [b] Calculated using a point charge model as described in ref 20.

to be 2.555 ± 0.010 eV, the lowest among all of the measured *M*(*x*,*y*) species. Our predicted values of 2.518 eV (B3LYP/6-31+G(d)) and 2.550 eV (CCSD(T)/6-311+G(3df,2p)) are in excellent accord with this result. Acid-catalyzed isomerization to the *M*(2,6) ion also may occur, but this conversion is nearly a thermoneutral process (−0.8 (B3LYP/6-31+G(d)) and −0.9 (CCSD(T)/6-311+G(3df,2p)) and the ADE for the rearranged species is 3.38 eV, so its signal would be buried under the higher binding *M*(2,7) features.

In summary, although the PES spectra of *D*(4,7)−CO_2, *D*(3,7)−CO_2, *D*(2,6)−CO_2, and probably *D*(2,3)−CO_2 appear

Table 6. Decarboxylation Energies of *D*(*x*,*y*) Zwitterions and Isomerization Energies of *M*(*x*,*y*) Anions[a]

D(x,y)	*M*(x,y)	Δ*H*°	isomerization energy[b]
2,3	2,3	32.4	
	3,2	25.5	−16.9 (−19.2, −16.7)[c]
2,4	2,4	40.8	
	4,2	30.0	−6.1 (−8.6, −5.1)[d]
2,5	2,5	40.9	
	5,2	30.3	−1.2 (−4.1, −0.6)[c]
2,6	2,6	29.2	+0.8 (−1.8, +0.9)[e]
2,7	2,7	23.4	
	7,2	26.5	
3,4	3,4	36.1	−33.0 (−35.4, −33.3)[c]
	4,3	32.6	−30.0 (−32.1, −31.1)[d]
3,5	3,5	39.1	−17.9 (−20.6, −17.9)[c]
3,7	3,7	26.2	
	7,3	38.6	
4,7	4,7	25.4	
	7,4	39.4	
2-*N*-$CH_3PyrCO_2^-$		15.4	
3-*N*-$CH_3PyrCO_2^-$		23.6	
4-*N*-$CH_3PyrCO_2^-$		24.2	

[a] All values in kcal mol^{-1}. [b] Energies in parentheses are at the B3LYP/6-311+G(2df,2pd) and CCSD(T)/6-311+G(3df,2p) levels, respectively. [c] *M*(3,7) is the product ion. [d] *M*(4,7) is the product ion. [e] *M*(2,7) is the product ion.

Scheme 3

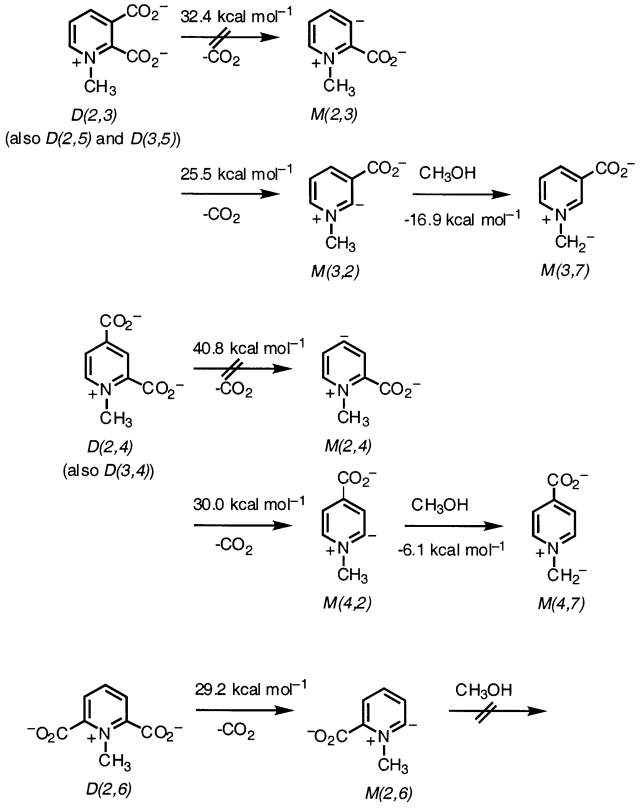

Scheme 4

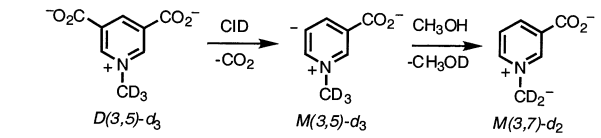

to be only due to *M*(4,7), *M*(3,7), *M*(2,6), and *M*(3,7), respectively, the rest of the spectra contain at least two components from different isomers (i.e., *M*(4,7) and *M*(3,7) for *D*(3,4)−CO_2, *M*(4,2) and *M*(4,7) for *D*(2,4)−CO_2, *M*(2,7) and

M(7,2) for *D*(2,7)−CO_2, *M*(3,5) and *M*(3,7) for *D*(3,5)−CO_2, and *M*(5,2) and *M*(3,7) for *D*(2,5)−CO_2). The coexistence of these isomers helps to account for the variation in the highest binding energy features of these species.

Optimized Structures of the *M*(*x*,*y*) Zwitterions. Most of the *M*(*x*,*y*) anions were found to have C_1 symmetry, but some of them (*M*(2,3), *M*(2,7), *M*(4,2), *M*(4,7), and *M*(5,2)) have a mirror plane containing the aromatic ring. Their most notable structural feature is intramolecular hydrogen bonding between the oxygen atom(s) of the carboxylates and the nearby methyl and aryl hydrogen atoms. These interactions are shown in Figure 6 and vary in distance from 1.963 to 2.970 Å (Table 3). A second characteristic in these zwitterions is the different orientations of the carboxylate groups. Those that are in the 3- and 4-positions adopt either a pseudo-planar orientation, in which there is conjugation between the π-system of the aromatic ring and the carboxylate group, or a twisted geometry. These variations occur, in part, because of the small Ph-CO_2^- rotational barrier in benzoate anion (i.e., 4.0 kcal mol^{-1} at the B3LYP/6-31+G(d) level). As for the 2-substituted carboxylates, they are all rotated out of the pseudo ring plane and hydrogen bond with the *N*-methyl group except for the *M*(2,7) anion, which is fully planar and has particularly short O−H distances of 1.963 and 2.253 Å. Finally, the *M*(4,3) ion is predicted to have a distorted aromatic ring at the B3LYP/6-31+G(d), MP2/6-31+G(d), and MP3/6-31+G(d) levels with out-of-plane dihedral angles as large as 15.2° (B3LYP), 12.3° (MP2), and 8.8° (MP3).

Comparison of Computed ADEs to Experimental and Calculated Relative *M*(*x*,*y*) Stabilities. The ADEs calculated at the B3LYP level with the 6-31+G(d) basis set are in excellent accord with experiment but are consistently too small by 0.076−0.175 eV (Table 4). These discrepancies can be reduced to 0.037−0.136 eV by accounting for the computed error in the electron binding energy of the phenyl anion (0.039 eV). In either case, these results are significantly better than for the *D*(*x*,*y*) zwitterions, which have absolute errors of ∼0.5 eV and corrected errors of ∼0.3 eV.[21] The reason for this difference in seemingly similar compounds is unclear at this time. ADEs also were computed for all 16 *M*(*x*,*y*) ions with the larger 6-311+G(2df,2pd) basis set. These more time intensive computations have little impact on the results (≤0.08 eV), but the ADEs are systematically smaller than those from the 6-31+G(d) data and are in poorer accord with the experiment. Consequently, these larger basis set calculations will not be discussed further.

Additional calculations using coupled-cluster theory were carried out to compare the computationally less demanding density function theory results with the high-level ab initio data at the CCSD(T)/6-311+G(3df,2p) level. The latter energies were obtained via an additivity scheme (see the Experimental Section) in an analogous fashion to G2 and G3 theory[55,56] because the molecules of interest are too large to carry out the computations directly. The B3LYP and CCSD(T) relative energies of the *M*(*x*,*y*) zwitterions and their predicted electron binding energies are in excellent accord with each other, and the CCSD(T) ADEs also are in excellent agreement with the experimentally determined values (errors ≤ 0.058 eV). Austin model 1 (AM1) semiempirical calculations[62] and Coulomb's law were used to explore the relative stabilities of the *M*(*x*,*y*) ions, too (Table 5). There is reasonable qualitative agreement between the different methods as we previously noted for the *D*(*x*,*y*) anions,[20,21] but, not surprisingly, the AM1 and Coulomb's law energies are not quantitatively useful. Given their much greater computational efficiency, however, these two methods should be useful when dealing with larger dipolar ions.

Table 7. Mulliken Population Spin Densities and Atomic Charges of the *M*(*x*,*y*) Radicals at the CO_2 and Aryl Anion (Radical) Centers[a]

	x (CO_2)		y (Ar)	
M(*x*,*y*)	spin	charge	spin	charge
M(2,3)	0.08	−0.63	1.01	0.11
M(3,2)	0.30	−0.24	0.60	0.20
M(2,4)	0.07	−0.68	0.99	−0.14
M(4,2)	0.22	−0.52	0.76	0.09
M(2,5)	0.00	−0.70	0.99	−0.05
M(5,2)	0.01	−0.70	0.97	0.22
M(2,6)	0.11	−0.62	0.89	0.19
M(3,4)	0.12	−0.56	0.96	0.17
M(4,3)	0.17	−0.35	0.87	0.29
M(3,5)	0.13	−0.62	0.90	−0.14
M(2,7)	0.03	−0.63	0.85	0.31
M(7,2)	0.09	−0.41	0.86	0.22
M(3,7)	0.02	−0.52	0.89	0.28
M(7,3)	0.17	−0.41	1.00	0.11
M(4,7)	0.19	−0.54	0.80	0.22
M(7,4)	−0.01	−0.43	0.97	−0.37

[a] Computed structures are at the B3LYP/6-31+G(d) level. Combined spin densities and atomic charges for the CO_2 group.

Mulliken Population Analyses. To verify that the photodetached electrons come from the aryl anion center upon irradiation of the *M*(*x*,*y*) anions, we examined the Mulliken population analysis of all of the corresponding radicals (Table 7). As expected, given the difference in the ADEs of phenyl anion[57] and benzoate[59] (1.096 vs 3.70 eV), both the spin densities and the atomic charges indicate that the ejected electron comes from the carbanion center. Only for the *M*(3,2) and *M*(4,2) ions, where the aryl anion is adjacent to the formal positive charge center and the carboxylate is more remote, does it appear that the odd electron maybe delocalized to an appreciable extent over the carboxylate group.

Mechanistic Implications for Orotidine 5′-Monophosphate Decarboxylase (ODCase). Decarboxylation of *D*(*x*,*y*) zwitterions can be viewed as a simple electrostatic model for the proposed enzyme-catalyzed expulsion of carbon dioxide from protonated orotidine 5′-monophosphate at either oxygen-2 or oxygen-4. To our surprise, the energetics for the former process at the 2-, 3-, and 4-positions are insensitive to the location of the second carboxylate group. That is, the reaction energies for the formation of *M*(*x*,2) anions span only a 4.8 kcal mol^{-1} range (25.5−30.3 kcal mol^{-1}), whereas those for the *M*(*x*,3) and *M*(*x*,4) ions differ by 8.5 and 4.7 kcal mol^{-1}, respectively (Table 6). The relative ordering in each group, as expected, correlates, in general, with the carbon−carbon distance between the two carboxylates. As for the magnitude of the decarboxylation energies, they all are larger than if the second carboxylate group were absent by anywhere from 9 to 17 kcal mol^{-1} (i.e., the reaction energies for 2-, 3-, and 4-*N*-methylpyridinium carboxylate are 15.4, 23.6, and 24.2 kcal mol^{-1}, respectively). In other words, the expulsion of carbon dioxide is retarded by the presence of a second carboxylate and its exact location is not

(62) Dewar, M. J. S.; Zoebisch, E. G.; Healy, E. F.; Stewart, J. J. P. *J. Am. Chem. Soc*. **1985**, *107*, 3902−3909.

overly important. Consequently, *the presence of an anionic center tends to counteract the benefit of zwitterion formation*.[63]

We also examined the effect of a remote negatively charged group on the decarboxylation of 1-methylorotate and its O4-protonated analogue (eq 3). Fluoride was used as the anion,

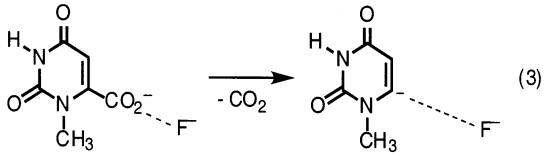

(3)

but this choice should not effect the qualitative picture because electrostatic interactions dominate. When F^- is held 4 Å from the carboxylate carbon in 1-methylorotate along the $C-CO_2$ axis, the decarboxylation is facilitated by 6.0 kcal mol^{-1}, whereas the expulsion of carbon dioxide from the O4-protonated structure is retarded by 4.4 kcal mol^{-1}.[64] The former result is amplified as fluoride is brought closer to the carboxylate group as one would expect (i.e., the decarboxylation is facilitated by 8.0, 10.2, 12.8, and 16.1 kcal mol^{-1} at distances of 3.75, 3.5, 3.25, and 3.0 Å, respectively). In contrast, the retardation of the protonated compound diminishes (3.2, 2.2, 0.6, and −1.0 kcal mol^{-1}, respectively) as F^- approaches the neutral substrate and starts to form an energetically favorable gas-phase ion−molecule complex. This latter interaction makes it difficult to model the reaction of the protonated substrate and limits the quantitative utility of these computations. Nevertheless, these findings are in keeping with the results on the *D*(*x*,*y*) zwitterions and indicate that the additionally charged group diminishes the electric field at the positively charged nitrogen center (i.e., the electrostatic driving force is reduced).

Four recent X-ray structure determinations of ODCase have been reported, and they all indicate that the carboxylic acid of an aspartic acid residue (Asp[70] in the enzyme from *Methanobacterium thermoautotrophicum*) is in close proximity to the carboxylate in OMP.[39−42] This amino acid is part of a conserved Asp-Lys-Asp-Lys tetrad, which is essential for catalysis.[65] If this aspartic acid is replaced by an alanine, however, then a chloride ion is brought in from the buffer and occupies the site of the missing carboxyl group.[66] This result and others indicate that a negatively charged group in the reaction region of substrate-bound ODCase is required for catalysis, but this point has been questioned.[67] Our findings suggest that if the aspartic acid is deprotonated (something we think is likely), then zwitterion formation as illustrated in Scheme 1 provides less of a driving force than currently thought. This does not mean that these pathways can be excluded because the decarboxylation could be further accelerated, for example, by making use of the hydrophobic effect. No such additional constraints are needed for the electrostatic stress mechanism (Scheme 2) put forth by Larsen et al.[42] and Pai, Guo, and co-workers,[39] and to this extent the latter proposal maybe more likely, although it certainly is controversial. In the nonenzymatic reaction, additional charged groups are not present and the zwitterion-stabilized process as originally suggested by Beak and Siegel,[28] or later modified by Lee and Houk,[32] undoubtedly, is followed. This latter pathway, however, may well be a "red herring" from a biological standpoint, which would be in keeping with forceful arguments put forth by Dewar slightly more than a quarter of a century ago.[68]

Conclusions

The decarboxylation of nine isomeric pyridinium dicarboxylate zwitterions (*D*(*x*,*y*)) was examined by photoelectron spectroscopy. Isotopic labeling experiments, independent syntheses, and comparison to extensive computations revealed that all of the ring-containing *D*(*x*,*y*) dicarboxylates except possibly the *D*(2,6) isomer undergo, at least in part, an acid-catalyzed isomerization following the loss of carbon dioxide. Adiabatic and vertical detachment energies for *M*(2,6), *M*(2,7), *M*(3,5), *M*(3,7), and *M*(4,7) were measured and span a range of 0.8 eV from 2.555 eV (*M*(2,7)) to 3.38 eV (*M*(2,6)). Vibrationally resolved data for all of these species except the highest binding energy isomer also were obtained.

Fully optimized B3LYP structures were computed for all 16 possible *M*(*x*,*y*) zwitterions. Their adiabatic electron detachment energies were subsequently calculated at the B3LYP level with the 6-31+G(d) and 6-311+G(2df,2pd) basis sets as well as via coupled-cluster theory (i.e., CCSD(T)/6-311+G(3df,2p)). In contrast to our previous work on the *D*(*x*,*y*) dicarboxylates, excellent agreement between experiment and theory (i.e., <0.14 eV) is obtained in all three cases. Semiempirical AM1 calculations and the application of Coulomb's law to the relative energies of the *M*(*x*,*y*) ions were found to be qualitatively useful, and this should be helpful when dealing with larger biologically interesting substrates. Finally, Mulliken population analyses of all of the *M*(*x*,*y*) radicals were carried out, and as expected they indicate that the photoejected electron predominantly comes from the carbanion center rather than the carboxylate group.

The expulsion of carbon dioxide from a carboxylate-containing molecule is facilitated by the introduction of a nearby positive charge center (i.e., zwitterion formation).[63] This effect has been used to rationalize the decarboxylation of OMP analogues in aqueous solution and is the basis of a mechanistic proposal for the enzyme-catalyzed reaction. Our results show that an additional anionic group serves to mitigate the energetic benefit of zwitterion formation, almost regardless of where the negative charge center is located. To the extent that a negatively charged aspartate is near the OMP carboxylate and that this amino acid is catalytically important, it seems that the phenomenal rate acceleration brought about by ODCase may be due to electrostatic stress, althought zwitterion formation certainly cannot be ruled out at this point.

Acknowledgment. This work was carried out in part while S.R.K. was a Visiting Fellow at the Australia National Univer-

(63) It is worth noting that the decarboxylation energies of 2-, 3-, and 4-pyridinecarboxylate are 54.1, 53.4, and 52.7 kcal mol^{-1}, respectively, and that *N*-methylation facilitates this process by 38.7, 29.8, and 28.5 kcal mol^{-1}, respectively. In all three cases this energetic gain is larger than the 23 kcal mol^{-1} activation that has been found for OMP in refs 25 and 27.

(64) These single-point energy calculations were carried out using B3LYP/6-31+G(d) fully optimized structures for 1-methylorotate, the corresponding vinyl carbanion of 1-methyluracil, and their O-4 protonated analogues; initial HF/6-31+G(d) geometries for these species were obtained from Phillips and Lee in ref 44. In the decarboxylated ions the F^-−vinyl carbon distance was kept the same as in the 1-methylorotates, and the fluoride ion bisected the N1−C6−C5 bond angle and was placed in the plane defined by these three atoms.

(65) Miller, B. G.; Snider, M. J.; Wolfenden, R.; Short, S. A. *J. Biol. Chem.* **2001**, *276*, 15174−15176.

(66) Wu, N.; Gillon, W.; Pai, E. F. *Biochemistry* **2002**, *41*, 4002−4011.

(67) Lee, T.-S.; Chong, L. T.; Chodera, J. D.; Kollman, P. A. *J. Am. Chem. Soc.* **2001**, *123*, 12837−12848.

(68) Dewar, M. J. S. *Enzyme* **1986**, *36*, 8−20.

sity. S.RK. thanks Prof. L. Radom for helpful discussions and making generous amounts of computer time at the ANU Supercomputing Facility available to us. We acknowledge Drs. D. Henry, A. Scott, and M. Sullivan for their computational assistance, particularly with regard to the MOLPRO program. We are grateful for support from the National Science Foundation, the donors of the Petroleum Research Foundation, as administered by the American Chemical Society, and the Minnesota Supercomputer Institute. This work also was performed in part at the W. R. Wiley Environmental Molecular Science Laboratory, a national scientific user facility sponsored by Department of Energy's Office of Biological and Environmental Research and located at Pacific Northwest National Laboratory, which is operated for the U.S. Department of Energy by Battelle.

Supporting Information Available: Computed structures and energetics (PDF). This material is available free of charge via the Internet at http://pubs.acs.org.

JA0290835